

# Driven transport of soft Brownian particles through pore-like structures: Effective size method

Alexander P. Antonov,<sup>1, a)</sup> Artem Ryabov,<sup>2, b)</sup> and Philipp Maass<sup>1, c)</sup>

<sup>1)</sup>*Universität Osnabrück, Fachbereich Physik, BarbarasträÙe 7, D-49076 Osnabrück, Germany*

<sup>2)</sup>*Charles University, Faculty of Mathematics and Physics, Department of Macromolecular Physics, V HoleÙoviÙkách 2, CZ-18000 Praha 8, Czech Republic*

(Dated: 29 May 2022)

Single-file transport in pore-like structures constitute an important topic for both theory and experiment. For hardcore interacting particles, a good understanding of the collective dynamics has been achieved recently. Here we study how softness in the particle interaction affects the emergent transport behavior. To this end, we investigate driven Brownian motion of particles in a periodic potential. The particles interact via a repulsive softcore potential with a shape corresponding to a smoothed rectangular barrier. This shape allows us to elucidate effects of mutual particle penetration and particle crossing in a controlled manner. We find that even weak deviations from the hardcore case can have a strong impact on the particle current. Despite of this fact, the knowledge about the transport in a corresponding hardcore system is shown to be useful to describe and interpret our findings for the softcore case. This is achieved by assigning a thermodynamic effective size to the particles based on the equilibrium density functional of hard spheres.

## I. INTRODUCTION

Understanding transport through pore-like structures is important for many chemical and biophysical processes and applications. Examples include pores of zeolites in catalysis,<sup>1</sup> carbon nanotubes with relevance to biotechnological and biomedical applications,<sup>2</sup> and particle motion in nanofluidic devices,<sup>3</sup> which can be utilized for various needs as water filtration and osmotic energy conversion.

Frequently the confining environment for the particle transport has a periodic structure that in theoretical modelings is most easily accounted for by an external periodic potential with wavelength  $\lambda$ . This potential can be of entropic origin, e.g., reflecting variations in a pore cross section,<sup>4–6</sup> or/and of energetic nature, e.g., when associated with binding sites inside a membrane channel.<sup>7–9</sup>

If the pore size is comparable to the particle diameter, the particle motion often has single-file character.<sup>10–16</sup> This means that the particles involved in the transport cannot pass each other and thus keep their ordering. The no-passing condition has severe implications on the dynamics. This was first realized in connection with anomalous subdiffusion of tracers<sup>17</sup> and a large number of studies has then been devoted to that problem.<sup>18–25</sup>

Recently it has been shown that the single-file constraint gives rise also to intriguing collective transport properties of Brownian particles in periodic potentials.<sup>26–28</sup> For hardcore interacting particles, this model was termed Brownian asymmetric simple exclusion process (BASEP), as it could be considered as a generalization of the asymmetric simple exclusion process (ASEP),<sup>29–31</sup> which is a paradigmatic lattice model for nonequilibrium dynamics. In the BASEP, the transport properties depend sensitively on the particle diameter  $\sigma$ . A

rich variety of current-density relations was found, which are known also as “fundamental diagrams”.<sup>32</sup> This rich variety causes complex diagrams of many nonequilibrium phases to emerge that are characterized by different types of steady states appearing in open systems coupled to particle reservoirs.

Here we study how collective transport properties are influenced if the interaction potential is not the ideal hardcore but exhibits some softness. This applies, for example, to the motion of interpenetrating macromolecules like polymer coils in a narrow channel. Or one can imagine hard-sphere colloidal particles to move in a channel slightly larger than their size. Instead of considering such situations in detail, we are interested here in a more generic treatment, where we focus on a rectangular barrier interaction potential with smoothed barrier steps.

Specifically, the particles interact via the pair potential

$$V(r) = \frac{V_0}{\varepsilon[1 + \operatorname{erf}(\sigma/\sqrt{2}\lambda\varepsilon)]} \operatorname{erfc}\left(\frac{r-\sigma}{\sqrt{2}\lambda\varepsilon}\right), \quad (1)$$

which is shown in Fig. 1(a). The variable  $r$  is the distance between the center positions of two particles and  $\sigma$  characterizes the particle size. The wavelength  $\lambda$  of the periodic potential appears in Eq. (1) just as a length scale. In fact, we will use it as length unit in the following, i.e.  $\lambda = 1$ . The parameter  $\varepsilon > 0$  is dimensionless and allows us to control the softness of the interaction. We refer to it as the softness parameter. With decreasing  $\varepsilon$ , the barrier edges become sharper and the interaction strength  $V_0/\varepsilon$  increases, see Fig. 1(a). In the limit  $\varepsilon \rightarrow 0$ , the hard-sphere potential for particles with diameter  $\sigma$  is recovered. We will speak about “hard particles” for  $\varepsilon = 0$  and about “soft particles” if  $\varepsilon > 0$ .

To describe the collective particle transport we focus on current-density relations, which we determine by extensive Brownian dynamics simulations. To explain our findings, we introduce an effective particle size for soft-particles based on equilibrium properties. This method bears some resemblance to an approach in the theory of simple fluids in equilibrium. Our effective size method applies to nonequilibrium transport

<sup>a)</sup>Electronic mail: alantonov@uos.de

<sup>b)</sup>Electronic mail: rjabov.a@gmail.com

<sup>c)</sup>Electronic mail: maass@uos.de

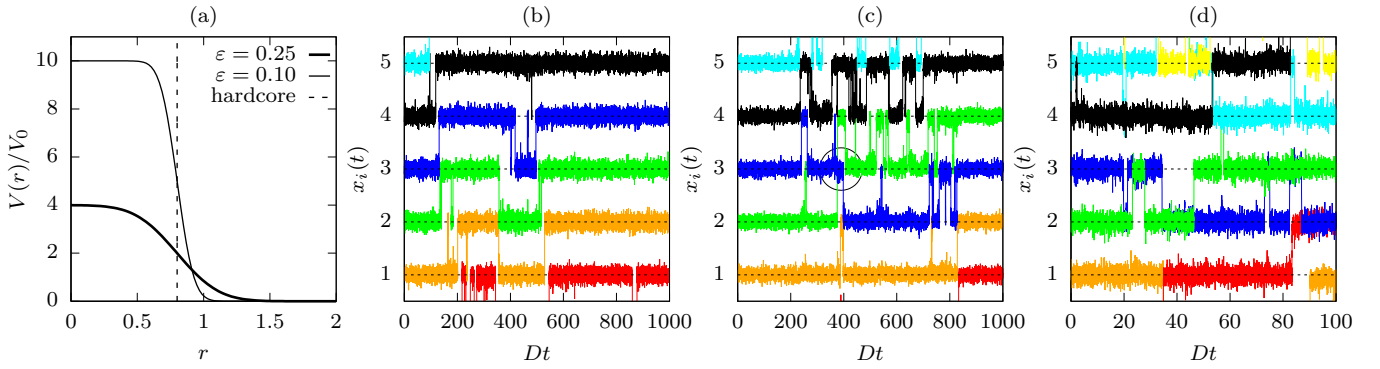


FIG. 1. (a) Interaction potential for soft particles of size  $\sigma = 0.8$  for two values of the softness parameter  $\varepsilon$ . The dashed line represents the hardcore potential in the limit  $\varepsilon \rightarrow 0$ . (b)-(d) Trajectories of driven Brownian motion through the cosine potential in Eq. (2) with barrier height  $U_0 = 6k_B T$  for a mean particle density  $\bar{\rho} = 0.8$  and particle size  $\sigma = 0.8$  under a constant drag force  $f/k_B T = 0.2$ . The amplitude  $V_0$  of the interaction potential is  $V_0 = k_B T$ . Panel (b) is for hard particles (BASEP), (c) for soft particles with  $\varepsilon = 0.1$  (low passing rate), and (d) for soft particles with  $\varepsilon = 0.25$  (high passing rate). The circle in panel (c) marks a crossing of two particles.

properties. It relies on the idea to use the system of hardcore interacting particles as a reference system for predicting collective dynamics of soft particles.

## II. MODEL

We consider an external cosine potential

$$U(x) = \frac{U_0}{2} \cos\left(\frac{2\pi x}{\lambda}\right) \quad (2)$$

with wavelength  $\lambda = 1$  and potential barriers  $U_0$  between wells much larger than the thermal energy  $k_B T$ . We use a fixed ratio  $U_0/k_B T = 6$ . The amplitude  $V_0$  of the interaction potential in Eq. (1) is set to  $k_B T$ . A constant drag force  $f$  is acting on all particles with  $f\lambda/k_B T = 0.2$ . The length  $L$  of the system is equal to 100 and periodic boundary conditions are applied. In the steady state, the particles are thus moving along a ring with a mean velocity in the direction of  $f$ .

For the pair potential in Eq. (1), the interaction force of a particle  $j$  at position  $x_j$  exerted on a particle  $i$  at position  $x_i$  is

$$\begin{aligned} f^{(2)}(x_i, x_j) &= -\frac{\partial V(|x_i - x_j|)}{\partial x_i} \\ &= \frac{\sqrt{2}V_0}{\sqrt{\pi}\varepsilon^2[1 + \operatorname{erf}(\sigma/\sqrt{2}\varepsilon)]} \\ &\quad \times \frac{x_i - x_j}{|x_i - x_j|} \exp\left(-\frac{(|x_i - x_j| - \sigma)^2}{2\varepsilon^2}\right). \end{aligned} \quad (3)$$

In the limit  $\varepsilon \rightarrow 0$  this force approaches a delta-function at the particle distance  $\sigma$  with amplitude  $V_0/\varepsilon$ . We will consider two values of  $\varepsilon$  in the following, namely  $\varepsilon = 0.1$  and  $\varepsilon = 0.25$  corresponding to a low and high passing rate, respectively. The interaction potential for these two  $\varepsilon$  values is displayed in Fig. 1(a).

The driven Brownian motion of  $N$  particles is described by

the Langevin equations

$$\frac{dx_i}{dt} = \mu \left( f - U'(x_i) + f_i^{\text{int}} \right) + \sqrt{2D} \xi_i(t), \quad i = 1, \dots, N, \quad (4)$$

where  $\mu$  is the particle mobility,  $D = k_B T \mu$  is the diffusion coefficient, and  $\xi_i(t)$  are Gaussian white noise processes with zero mean and correlation functions  $\langle \xi_i(t) \xi_j(t') \rangle = \delta_{ij} \delta(t - t')$ ;  $f_i^{\text{int}} = \sum_{j \neq i} f^{(2)}(x_i, x_j)$  is the total interaction force acting on particle  $i$  and  $U'(\cdot)$  is the derivative of the external potential.

The mean number density of particles is

$$\bar{\rho} = \frac{N}{L}. \quad (5)$$

Because we defined  $\lambda$  as our length unit, we can regard  $\bar{\rho}$  also as the filling factor  $N\lambda/L$ , i.e. mean number of particles per potential well.

We solved the Langevin equations (4) by applying the Euler discretization scheme with time steps  $D\Delta t = 10^{-5} - 10^{-4}$ . It was checked that our results are neither affected by the time step nor by the finite system length. For treating the hardcore interaction ( $\varepsilon = 0$ ) we followed the procedure proposed in Ref. 33 as described in detail in Ref. 27.

Figures 1(b), (c) and (d) show representative particle trajectories for hard particles [BASEP, panel (b)], and soft particles for low and high passing rate [panels (c) and (d)]. In all figures the density is  $\bar{\rho} = 0.8$  and the particles have size  $\sigma = 0.8$ . Following the trajectories, we see jump-like transitions between the potential wells, because the thermal energy  $k_B T$  is much smaller than the potential barrier  $U_0$ . While the particles keep their ordering (single-file motion) in Fig. 1(b), one particle crossing can be seen in the time window  $1000/D$  in Fig. 1(c). The corresponding event is marked by a circle. In Fig. 1(d), many more particle crossings occur even in a ten times smaller time window. In addition, we observe many particle overlaps as reflected in overlapping colors. This demonstrates that the potential for  $\varepsilon = 0.25$  is very soft.

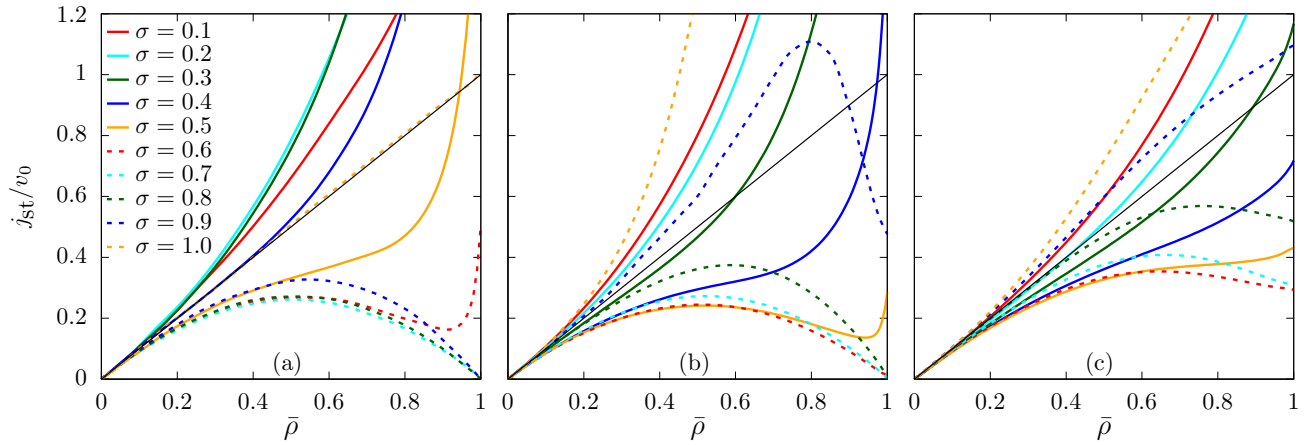


FIG. 2. Simulated current-density relations for various particle sizes. Panel (a) is for hard particles, and panels (b) and (c) are for soft particles with  $\varepsilon = 0.1$  and  $\varepsilon = 0.25$ , respectively. The legend in (a) applies to all panels. The current is normalized to the mean velocity  $v_0$  of a single particle and the thin solid line with slope one represents the behavior of independent particles in all panels.

We next discuss current-density relations (fundamental diagrams) in dependence of the particle size  $\sigma$  and mean density  $\bar{\rho}$  for two softness parameters  $\varepsilon = 0.1$  and  $\varepsilon = 0.25$ .

### III. DEPENDENCE OF CURRENTS ON DENSITY AND PARTICLE SIZE: SIMULATIONS

For independent particles, the current does not depend on  $\sigma$  and is given by  $j_0(\bar{\rho}) = v_0 \bar{\rho}$ , where  $v_0 = v_0(f)$  is the mean velocity of a particle, when it is dragged through the periodic potential  $U(x)$  by the force  $f$ . This mean velocity is known analytically<sup>34</sup> and we use it to normalize simulated currents. Normalized currents  $j_{\text{st}}(\bar{\rho}, \sigma)/v_0$  are shown in Fig. 2(a)-(c) as a function of the density for various fixed particles sizes  $\sigma$ . The current-density relations in Fig. 2(a) are for the hard particles ( $\varepsilon = 0$ ), and those in Figs. 2(b) and (c) are for the soft particles with  $\varepsilon = 0.1$  and  $\varepsilon = 0.25$ , respectively. The solid line with slope one in all graphs marks the current for independent particles.

The current-density relations for the BASEP in Fig. 2(a) have been investigated in our previous studies and serve as reference to discuss the impact of softness of the potential. In the BASEP, the change of the current with density for varying  $\sigma$  can be attributed to a barrier reduction and blocking effect that compete with each other. The blocking effect leads to a fundamental diagram reminiscent to that of the ASEP for particle sizes in a limited range  $0.65 \lesssim \sigma \lesssim 0.8$ . Outside this range, the behavior is more complex.

In addition, there is a scaling transformation for collective transport quantities under a rescaling of both  $\bar{\rho}$  and  $\sigma$ . For the current, this reads

$$j_{\text{st}}(\bar{\rho}, \sigma) = (1 - m\bar{\rho}) j_{\text{st}}\left(\frac{\bar{\rho}}{1 - m\bar{\rho}}, \sigma - m\right), \quad (6)$$

where  $m = \text{int}(\sigma)$  is the integer part of  $\sigma$ . Due to Eq. (6), the current behavior for  $\sigma \geq 1$  can be inferred from that for  $\sigma < 1$ . The relation also implies the surprising result that the

current for  $\sigma = 1$  is equal to that of independent particles, see the respective simulated line in Fig. 2(a).

In what follows it is important to note that Eq. (6) tells us that the current behavior drastically changes if  $\sigma$  is increased only very little from  $\sigma < 1$  to  $\sigma > 1$ . For  $\sigma < 1$ , the current becomes extremely small for  $\bar{\rho} \rightarrow 1$  (dominant blocking effect) while for  $\sigma > 1$ , the system actually corresponds to one with a small particle size ( $\sigma - 1$ ), where the barrier reduction effect prevails (large currents, including the current in the limit  $\bar{\rho} \rightarrow 1$ ).

For soft particles, the scaling transformation does not hold, because in deriving Eq. (6), it is assumed that the particles cannot overlap. Nevertheless, the relation (6) is very useful for understanding the transport behavior of soft particles. This will be shown in Sec. V A.

#### A. Low passing rate

For discussing how the current-density relations change for the soft particles, let us first focus on the case of low passing rate displayed in Fig. 2(b) ( $\varepsilon = 0.1$ ). The rather complex behavior of  $j_{\text{st}}(\bar{\rho}, \sigma)$  in this figure can be described as follows.

For small  $\sigma \lesssim 0.3$ , in analogy with the behavior in Fig. 2(a), the currents are dominated by the barrier reduction effect, which leads to an enhancement of  $j_{\text{st}}(\bar{\rho}, \sigma)$  in comparison to independent particles (for  $\sigma = 0.3$  the current is slightly smaller than  $v_0 \bar{\rho}$  in Fig. 2(b) for  $\bar{\rho} \lesssim 0.6$ ). The barrier reduction effect occurs because two (or more) particles can be in the same potential well. Their average positions inside the well then are displaced from the minimum, leading to a reduced barrier for surmounting the saddle points to the neighboring well. As the fraction of multiple occupied wells increases with  $\bar{\rho}$ , the enhancement of the current becomes stronger. This is reflected in the upward bending of the current curves for small sigma in Fig. 2(b) (and also for  $\sigma = 0.4$  and  $0.5$  at large  $\bar{\rho}$ ).

For intermediate  $0.4 \lesssim \sigma \lesssim 0.8$ , the current-density relations in Fig. 2(b) become influenced and eventually domi-

nated by the blocking effect, which causes the current to become reduced in comparison to that of independent particles. The blocking effect is well known in lattice models like the ASEP<sup>29–31</sup> and occurs because the motion of a particle from one well to the next is strongly hindered if the neighboring well is already occupied by a particle. In fact,  $j_{\text{st}}(\bar{\rho}, \sigma)/v_0$  is close to the parabolic form  $\bar{\rho}(1 - \bar{\rho})$  of the ASEP for  $\sigma = 0.6$  and  $0.7$  in Fig. 2(b).

A closer inspection of the current-density relations for both small and intermediate particle sizes in Figs. 2(a) and (b) reveals an interesting common pattern: The relations in Fig. 2(b) appear to be very similar to those in Fig. 2(a) if  $\sigma$  is shifted by about  $0.1$ . For example, the line for  $\sigma = 0.4$  in Fig. 2(b) corresponds to the line for  $\sigma = 0.5$  in Fig. 2(a). More generally, we can say that the lines for  $\sigma = 0.1 - 0.8$  in Fig. 2(b) correspond to the lines for  $\sigma = 0.2 - 0.9$  in Fig. 2(a), respectively. This suggests that the currents  $j_{\text{st}}(\bar{\rho}, \sigma)$  for the soft particles in the respective  $\sigma$  regime can be described by that of the hard particles with an effective particle size

$$\sigma' = \sigma'(\bar{\rho}, \sigma), \quad (7)$$

where the dependence of  $\sigma'$  on  $\bar{\rho}$  should be weak.

Remarkably, this similarity of the current-density behavior is no longer found for large  $\sigma \gtrsim 0.9$ . The curve for  $\sigma = 1$  displays an upward bending for the range of densities  $\bar{\rho} \lesssim 0.5$  covered in the figure, as if the blocking effect is irrelevant. One may conjecture that this curve can be interpreted in terms of an effective particle size  $\sigma'$  larger than one, which according to Eq. (6) would correspond to a small particle size. However, as discussed above, Eq. (6) can no longer be assumed to be valid for soft particles.

Even more surprising is the curve for  $\sigma = 0.9$ , which seems to have no counterpart in Fig. 2(a). The question arises: Is it possible to develop a procedure to determine an effective particle size as conjectured in Eq. (7) by which we can understand the results for soft particles based on that for hard particles? If this is true, the BASEP could serve as a reference system for driven Brownian transport through periodic potentials, similar as the hard-sphere fluid constitutes a proper reference system in the equilibrium theory of simple fluids.<sup>35</sup>

## B. High passing rate

The current-density relations for the high passing rate in Fig. 2(c) show features partly analogous to those in Fig. 2(b) for the low passing rate, but with much weaker sensitivity to  $\sigma$ . The higher probability of passing apparently causes both the barrier enhancement and the blocking effect to become weaker. As a consequence, the currents deviate less from that of independent particles. The currents for all  $\sigma$  exhibit appreciable values in the limit  $\bar{\rho} \rightarrow 1$  and fundamental diagrams reminiscent to that of the ASEP do no longer appear. The weakening of the blocking is responsible also for the fact that the curve for  $\sigma = 0.9$  does no longer show a maximum followed by a strong decrease with density as in Fig. 2(b).

## IV. THEORETICAL APPROACHES

### A. Effective size method

This approach rests on the idea that the BASEP can serve as a reference system: the current of the soft particles is given by that of the BASEP with the same particle density and an effective hardcore diameter  $\sigma'$ . To define  $\sigma'$ , we require the equilibrium density profile for the softcore interacting particles to agree as closely as possible with that of the corresponding hardcore interacting ones.

The equilibrium density profile for the hard-sphere interacting particles follows from minimizing the density functional<sup>36</sup>

$$\begin{aligned} \Omega_{\text{hc}}(\sigma_{\text{hc}}; [\rho]) & \\ &= \int_0^1 dx \rho(x) \left\{ U(x) - \mu_{\text{ch}} - k_{\text{B}}T \left[ 1 - \ln \left( \frac{\rho(x)}{1 - \eta(x, \sigma_{\text{hc}})} \right) \right] \right\}, \end{aligned} \quad (8a)$$

where

$$\eta(x, \sigma_{\text{hc}}) = \int_{x - \sigma_{\text{hc}}}^x dy \rho(y). \quad (8b)$$

The determining equation for  $\sigma'$  is given by

$$\sigma'(\bar{\rho}, \sigma) = \operatorname{argmin}_{\sigma_{\text{hc}}} \left\{ \sup_{0 \leq x \leq 1} \left| \frac{\delta \Omega_{\text{hc}}(\sigma_{\text{hc}}; [\rho_{\text{eq}}])}{\delta \rho_{\text{eq}}(x)} \right| \right\}. \quad (9)$$

This means that we insert the equilibrium density  $\rho_{\text{eq}}(x)$  of the soft particles with size  $\sigma$  and mean density  $\bar{\rho}$  into the functional derivative of  $\Omega_{\text{hc}}$  and vary  $\sigma_{\text{hc}}$  until we find that  $\sigma_{\text{hc}} = \sigma'$ , where  $|\delta \Omega_{\text{hc}}(\sigma_{\text{hc}}; [\rho_{\text{eq}}]) / \delta \rho_{\text{eq}}(x)|$  deviates by the smallest amount from zero in the interval  $0 \leq x \leq 1$ .

Having determined  $\sigma'(\bar{\rho}, \sigma)$  in this manner, the current is given by

$$j_{\text{st}}(\bar{\rho}, \sigma) = j_{\text{st}}^{\text{BASEP}}(\bar{\rho}, \sigma'), \quad (10)$$

where  $j_{\text{st}}^{\text{BASEP}}$  is the stationary current for the BASEP.

### B. Approximation of zero mean interaction force (AZMIF)

The continuity equation for the local density  $\rho(x, t) = \langle \sum_i \delta(x - x_i(t)) \rangle$  reads<sup>27</sup>

$$\begin{aligned} \frac{\partial \rho(x, t)}{\partial t} &= - \frac{\partial j(x, t)}{\partial x} \\ &= - \frac{\partial}{\partial x} \left[ \mu (f - U'(x) + f_{\text{int}}(x, t)) \rho(x, t) - D \frac{\partial \rho(x, t)}{\partial x} \right], \end{aligned} \quad (11)$$

where

$$f^{\text{int}}(x, t) = \frac{1}{\rho(x, t)} \int_0^L dy f^{(2)}(x, y) \rho^{(2)}(x, y, t) \quad (12)$$

is the local mean interaction force and  $\rho^{(2)}(x,y,t) = \langle \sum_{i=1}^N \sum_{k=1, k \neq i}^N \delta(x - x_i(t)) \delta(y - x_k(t)) \rangle$  is the two-particle density.

In the steady-state, the density profile and the mean interaction force are time-independent,  $\rho(x,t) = \rho_{\text{st}}(x)$  and  $f^{\text{int}}(x,t) = f_{\text{st}}^{\text{int}}(x)$ . The current becomes both time-independent and homogeneous,  $j(x,t) = j_{\text{st}}(\bar{\rho}, \sigma)$ . From Eq. (11) one then derives<sup>27</sup>

$$j_{\text{st}}(\bar{\rho}, \sigma) = \frac{f + \overline{f_{\text{st}}^{\text{int}}}}{\int_0^1 \frac{dx}{\rho_{\text{st}}(x)}}, \quad (13a)$$

where

$$\overline{f_{\text{st}}^{\text{int}}} = \int_0^1 dx f_{\text{st}}^{\text{int}}(x) \quad (13b)$$

is the period-averaged mean interaction force.

In the linear response limit for small drag force  $f$ , Eq. (13a) becomes

$$j_{\text{st}}(\bar{\rho}, \sigma) = \frac{1 + \alpha}{\int_0^1 \frac{dx}{\rho_{\text{eq}}(x)}} f, \quad (14a)$$

$$\alpha = \left. \frac{\partial \overline{f_{\text{st}}^{\text{int}}}}{\partial f} \right|_{f=0}, \quad (14b)$$

where  $\rho_{\text{eq}}(x)$  is the equilibrium density profile for  $f = 0$ .

The influence of the mean interaction force on the current in Eq. (14a) is given by the factor  $\alpha$ , which depends on  $\bar{\rho}$  and  $\sigma$ . To determine this factor would require a calculation of the two-particle density  $\rho_{\text{st}}^{(2)}(x,y)$  in the stationary state (for small  $f$ ). This is a very challenging task.

An approximation is obtained by neglecting the impact of  $\overline{f_{\text{st}}^{\text{int}}}$  on  $j_{\text{st}}(\bar{\rho}, \sigma)$ , corresponding to setting  $\alpha = 0$  in Eq. (14a). We referred to this approach as the ‘‘small-driving approximation’’ in our former studies,<sup>26–28</sup> but use the more precise designation ‘‘approximation of zero mean interaction force’’ (AZMIF) here.

## V. APPLICATION OF THEORETICAL APPROACHES AND INSIGHTS FROM EFFECTIVE SIZE METHOD

For the BASEP,<sup>27</sup> we have found earlier that the AZMIF could capture the variation of currents with density qualitatively and that a fair quantitative agreement was obtained for small and large particle sizes ( $\sigma \lesssim 0.3$  and  $\sigma \gtrsim 0.7$ ). For  $\sigma$  around half the wavelength of the periodic potential, the AZMIF gave a less good prediction. The theoretical description could not be improved by including information on pair correlation functions, when we extended the theoretical treatment by employing the dynamic density functional theory (DDFT). We applied the DDFT also to the soft particle system with a scheme as discussed in Ref. 27. Again the AZMIF and DDFT gave overall similar results and we therefore discuss in the following the outcomes of the AZMIF and effective size method.

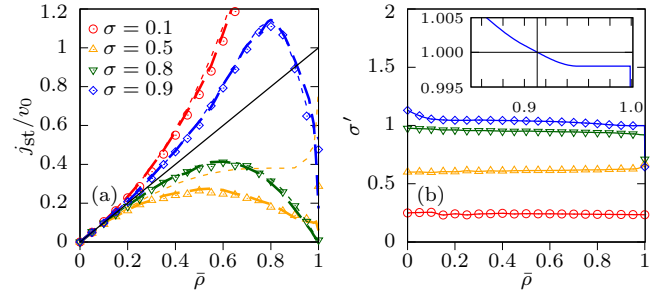


FIG. 3. (a) Comparison of current-density relations predicted by the AZMIF (thin dashed lines) and the effective size method (thick dashed line) with the simulated data (symbols) for low passing rate ( $\epsilon = 0.1$ ) and four representative particle sizes. The solid line with slope one indicates the behavior for independent particles. (b) Effective particle sizes calculated from Eq. (9) for the data shown in (a) [same symbols and line colors, see legend in part (a)]. The inset shows a zoom-in of the curve for  $\sigma = 0.9$  and  $\bar{\rho}$  close to one.

### A. Low passing rate

For the case of low passing ( $\epsilon = 0.1$ ), the behavior of  $j_{\text{st}}(\bar{\rho}, \sigma)$  predicted by the AZMIF (thin dashed lines) and effective size method (thick dashed lines) is shown in Fig. 3(a) in comparison with the simulated data. Similarly as in the BASEP, the AZMIF provides a good description for small and large particle sizes, but around  $\sigma = 0.5$  there appear pronounced differences, see the yellow symbols and corresponding thin dashed line in Fig. 3(a). In contrast, the effective size method gives a good description for all particle sizes.

The effective sizes  $\sigma' = \sigma'(\bar{\rho}, \sigma)$  are shown in Fig. 3(b) as a function of  $\bar{\rho}$  for the same  $\sigma$  as in Fig. 3(a). Note that the  $\sigma'$  were determined from Eq. (9) by using only equilibrium properties of the system. For  $\sigma \lesssim 0.8$ , as we expected in Sec. III A, the effective size  $\sigma'$  is by about 0.1 larger than  $\sigma$ . The variation with  $\bar{\rho}$  is weak, except in the limit  $\bar{\rho} \rightarrow 1$  at large  $\sigma$ .

The effective size method allows us now to understand the current-density relation for  $\sigma = 0.9$  in Fig. 2(b), which has no counterpart in current-density relations of the BASEP for any fixed particle size. As we discussed in Sec. III, for  $\sigma'$  close to one, even weak variations of  $\sigma'$  with  $\bar{\rho}$  can have a huge impact on the current-density relation. The inset in Fig. 3(b) shows a decrease of  $\sigma'$  from  $\sigma' > 1$  to  $\sigma' < 1$ , where  $\sigma' = 1$  at  $\bar{\rho}_\times \simeq 0.91$ . This means that the current of the soft particles should be dominated by the barrier-reduction effect for  $\bar{\rho} < \bar{\rho}_\times$ , equal to that of independent particles for  $\bar{\rho} \simeq \bar{\rho}_\times$ , and governed by the blocking effect for  $\bar{\rho} > \bar{\rho}_\times$ . Indeed, the fundamental diagram for  $\sigma = 0.9$  in Fig. 2(b) [or Fig. 3(a)] shows the corresponding features. In the limit  $\bar{\rho} \rightarrow 1$ , the current for the soft particles is not approaching zero (or very small values) as in the BASEP [see Fig. 2(a)] because the blocking effect is weaker. Surprisingly, this different limiting behavior for  $\bar{\rho} \rightarrow 1$  is captured qualitatively by a jump-like decrease of  $\sigma'$  in the effective size method, see the inset in Fig. 3(b).

However, contrary to the currents for  $\bar{\rho} < 1$ , it is very difficult to obtain reliable quantitative predictions of the currents

for  $\bar{\rho} = 1$  if  $\sigma' \gtrsim 0.4$ . The reason for this is that the current in the BASEP for  $\bar{\rho} = 1$  is strongly decreasing with particle size by several orders of magnitude for  $\sigma \gtrsim 0.4$ . Hence, even small numerical errors in the determination of  $\sigma'$  can lead to a large change of the predicted current. Also, the simulated BASEP currents in the respective regime are difficult to determine with the required accuracy.

The large soft-particle current for  $\sigma = 1$  in Fig. 2(b) with its upward bending for  $\bar{\rho} \lesssim 0.5$  can be explained by the effective size method as well. In this case,  $\sigma'$  is slightly larger than one [not shown in Fig. 3(b)], implying that the currents correspond to ones for hard particles with small size ( $\sigma' - 1$ ) according to the transformation (6). Hence, the barrier-reduction prevails and we see the corresponding behavior in Fig. 2(b).

One can explain the dominance of the barrier reduction effect for  $\sigma' \gtrsim 1$  also without using the transformation (6). Imagine two particles with  $\sigma' \gtrsim 1$  occupying neighboring wells. These cannot be at the minima of the potential at the same time, i.e. they are on average displaced from the bottom of the wells. Accordingly, they need less energy to overcome the saddle point to a vacant neighboring well. Because the number of particles occupying neighboring wells increases with the density, the corresponding enhancement of the current becomes stronger with  $\bar{\rho}$ , leading to the upward bending of the current-density relations.

## B. High passing rate

For the very soft particles ( $\varepsilon = 0.25$ ), one should expect the effective size method to be less appropriate. At high densities, in particular, neighboring particles can easily “overlap”, see also Fig. 1(d). Nevertheless, as shown in Fig. 4, the effective size method (thick dashed lines) still predicts many features correctly. For  $\sigma = 0.8$ , the current-density relation is surprisingly well predicted when  $\bar{\rho} < 1$ . If  $\bar{\rho} = 1$ , the effective size method suffers from the same problems as already discussed in Sec V A.

Also the simulated current-density relations (symbols) for  $\sigma = 0.1$  and  $\sigma = 0.9$  are quite well described for  $\bar{\rho} \lesssim 0.7$  by the effective size method, whereas at larger  $\bar{\rho}$  stronger deviations are seen due to increased particle overlappings. For  $\sigma = 0.5$ , significant deviations set in already at  $\bar{\rho} \simeq 0.5$ . This is likely related to a stronger mean interaction force  $\overline{f_{st}^{int}}$  in this regime [see Eqs. (13a), (14a)], which facilitates particle overlapping. That the mean interaction force must be strong at  $\sigma = 0.5$  can be seen from the failure of the AZMIF (thin dashed lines) to predict the current-density relation. This is reminiscent to the behavior in the BASEP,<sup>27</sup> where  $\overline{f_{st}^{int}}$  is also particularly large around  $\sigma = 0.5$ . In contrast to the case of low passing rate, the AZMIF for the other  $\sigma$  values yields predictions comparable to the effective size method.

## VI. SUMMARY AND CONCLUSIONS

We have studied Brownian motion of particles through a cosine potential under a constant drag force as a model for

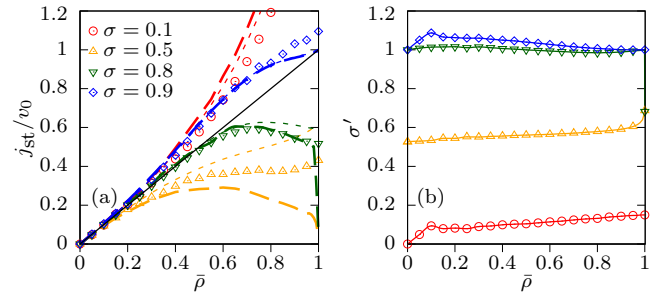


FIG. 4. (a) Comparison of current-density relations predicted by the AZMIF (thin dashed lines) and the effective size method (thick dashed line) with the simulated data (symbols) for high passing rate ( $\varepsilon = 0.25$ ) and the same particle sizes as in Fig. 3. The solid line with slope one indicates the behavior for independent particles. (b) Effective particle sizes calculated from Eq. (9) for the data shown in (a) [same symbols and line colors, see legend in part (a)].

driven diffusive transport through pore-like structures. Our aim was to explore how a softness in the particle interaction affects collective transport properties. To allow for a systematic comparison with hardcore interacting particles, we considered the interaction to be given by a smoothed rectangular barrier potential whose softness could be tuned by a single parameter.

The softness of this potential brings about two features: a smoothed barrier step and a finite height of the barrier. The smoothed step causes particles to partially penetrate each other (penetration effect) and the finite barrier allows particles to pass each other (passing effect). We focused our analysis on two cases of low and high passing rate. In the case of low passing rate, only the penetration effect is essentially present.

Even if the passing rate is negligible, we found peculiar current-density relations having no counterpart in a hardcore interacting system. To explain this, we introduced an effective particle size method. In this method, we map a system of softcore interacting particles onto that of hardcore interacting ones with the same density and an effective hardcore diameter that is determined based on the equilibrium density functional of hard spheres. This effective hardcore diameter depends on both the size and density of the soft particles and due to this dependence, the peculiar current-density relations could be well described. We can conclude therefore that the effective size method accounts correctly for the impact of the penetration effect on the transport behavior. In addition it allows one to interpret the dynamics based on the knowledge about the hardcore interacting reference system.

If the potential barrier is low, the passing rate of particles can become important. In this case there exist two regimes, one at low density, where the penetration effect prevails and another one at high density where the passing effect is dominant. In the low-density regime, the current-density relation can thus be successfully described by our effective size method. In the high-density regime, the effective size method does no longer provide a good quantitative description. Apparently, a different or modified theoretical approach is needed to cope with the collective dynamics in that regime.

The effective size method has been applied here to describe current-density relations as a fundamental aspect of nonequilibrium dynamics. We expect it to apply also to other nonequilibrium properties. Moreover, the method could be a valuable approach for treating soft particles with long-range attractive interactions.<sup>37</sup> To determine the effective size in that case, advancements of equilibrium density functional theory for corresponding hardcore interacting systems are useful.<sup>38,39</sup> Likewise, mixtures of soft particles may be treated based on density functionals for hard sphere mixtures.<sup>40,41</sup> As for experimental verification of the findings reported here, it is important to point out that the striking effects in the collective transport can not only be identified in currents but also in the local kinetics of tagged particles.<sup>42,43</sup>

## ACKNOWLEDGMENTS

Financial support by the Czech Science Foundation (Project No. 20-24748J) and the Deutsche Forschungsgemeinschaft (Project No. 432123484) is gratefully acknowledged.

- <sup>1</sup>M. Van de Voorde and B. Sels, eds., *Nanotechnology in Catalysis: Applications in the Chemical Industry, Energy Development, and Environment Protection* (Wiley-VCH, Weinheim, 2017).
- <sup>2</sup>S. Zeng, J. Chen, X. Wang, G. Zhou, L. Chen, and C. Dai, "Selective transport through the ultrashort carbon nanotubes embedded in lipid bilayers," *J. Phys. Chem. C* **122**, 27681–27688 (2018).
- <sup>3</sup>M. Ma, F. Grey, L. Shen, M. Urbakh, S. Wu, J. Z. Liu, Y. Liu, and Q. Zheng, "Water transport inside carbon nanotubes mediated by phonon-induced oscillating friction," *Nat. Nanotechnol.* **10**, 692 (2015).
- <sup>4</sup>K. K. Mon and J. K. Percus, "Pore-size dependence of quasi-one-dimensional single-file diffusion mobility," *J. Phys. Chem. C* **111**, 15995–15997 (2007).
- <sup>5</sup>P. S. Burada, P. Hänggi, F. Marchesoni, G. Schmid, and P. Talkner, "Diffusion in confined geometries," *ChemPhysChem* **10**, 45–54 (2009).
- <sup>6</sup>M. Mangeat, T. Guérin, and D. S. Dean, "Dispersion in two-dimensional periodic channels with discontinuous profiles," *J. Chem. Phys.* **149**, 124105 (2018).
- <sup>7</sup>C. Hilty and M. Winterhalter, "Facilitated substrate transport through membrane proteins," *Phys. Rev. Lett.* **86**, 5624–5627 (2001).
- <sup>8</sup>J. J. Kasianowicz, T. L. Nguyen, and V. M. Stanford, "Enhancing molecular flux through nanopores by means of attractive interactions," *PNAS* **103**, 11431–11432 (2006).
- <sup>9</sup>S. D. Goldt and E. M. Terentjev, "Role of the potential landscape on the single-file diffusion through channels," *J. Chem. Phys.* **141**, 224901 (2014).
- <sup>10</sup>M. Hartmann, "Ordered mesoporous materials for bioadsorption and biocatalysis," *Chem. Mater.* **17**, 4577–4593 (2005).
- <sup>11</sup>H. H. P. Yiu, C. H. Botting, N. P. Botting, and P. A. Wright, "Size selective protein adsorption on thiol-functionalised sba-15 mesoporous molecular sieve," *Phys. Chem. Chem. Phys.* **3**, 2983–2985 (2001).
- <sup>12</sup>B. Hille, *Ionic Channels of Excitable Membranes*, 3rd ed. (Sinauer Associates, Sunderland MA, 2001).
- <sup>13</sup>K. Hahn, J. Kärger, and V. Kukla, "Single-file diffusion observation," *Phys. Rev. Lett.* **76**, 2762–2765 (1996).
- <sup>14</sup>C. Chmelik, J. Caro, D. Freude, J. Haase, R. Valiullin, and J. Kärger, "Diffusive Spreading of Molecules in Nanoporous Materials," (Springer International Publishing, Cham, 2018) Chap. 10, pp. 171–202.
- <sup>15</sup>C.-Y. Cheng and C. R. Bowers, "Observation of single-file diffusion in dipeptide nanotubes by continuous-flow hyperpolarized Xenon-129 NMR spectroscopy," *ChemPhysChem* **8**, 2077–2081 (2007).
- <sup>16</sup>M. Dvoyashkin, H. Bhave, N. Mirzazari, S. Vasenkov, and C. R. Bowers, "Single-file nanochannel persistence lengths from NMR," *Anal. Chem.* **86**, 2200 (2014).
- <sup>17</sup>T. E. Harris, "Diffusion with "collisions" between particles," *J. Appl. Probab.* **2**, 323–338 (1965).
- <sup>18</sup>L. Lizana and T. Ambjörnsson, "Single-file diffusion in a box," *Phys. Rev. Lett.* **100**, 200601 (2008).
- <sup>19</sup>A. Taloni, A. Chechkin, and J. Klafter, "Generalized elastic model yields a fractional Langevin equation description," *Phys. Rev. Lett.* **104**, 160602 (2010).
- <sup>20</sup>A. Ryabov and P. Chvosta, "Single-file diffusion of externally driven particles," *Phys. Rev. E* **83**, 020106 (2011).
- <sup>21</sup>L. P. Sanders and T. Ambjörnsson, "First passage times for a tracer particle in single file diffusion and fractional Brownian motion," *J. Chem. Phys.* **136**, 175103 (2012).
- <sup>22</sup>A. Ryabov, "Single-file diffusion in an interval: First passage properties," *J. Chem. Phys.* **138**, 154104 (2013).
- <sup>23</sup>N. Leibovich and E. Barkai, "Everlasting effect of initial conditions on single-file diffusion," *Phys. Rev. E* **88**, 032107 (2013).
- <sup>24</sup>T. Ooshida, S. Goto, and M. Otsuki, "Collective motion of repulsive Brownian particles in single-file diffusion with and without overtaking," *Entropy* **20**, 565 (2018).
- <sup>25</sup>R. Wittmann, H. Löwen, and J. M. Brader, "Order-preserving dynamics in one dimension – single-file diffusion and caging from the perspective of dynamical density functional theory," *Mol. Phys.* **0**, e1867250 (2021).
- <sup>26</sup>D. Lips, A. Ryabov, and P. Maass, "Brownian asymmetric simple exclusion process," *Phys. Rev. Lett.* **121**, 160601 (2018).
- <sup>27</sup>D. Lips, A. Ryabov, and P. Maass, "Single-file transport in periodic potentials: The Brownian asymmetric simple exclusion process," *Phys. Rev. E* **100**, 052121 (2019).
- <sup>28</sup>D. Lips, A. Ryabov, and P. Maass, "Nonequilibrium transport and phase transitions in driven diffusion of interacting particles," *Z. Naturforsch. A* **75**, 449 (2020).
- <sup>29</sup>B. Derrida, "An exactly soluble non-equilibrium system: The asymmetric simple exclusion process," *Phys. Rep.* **301**, 65 – 83 (1998).
- <sup>30</sup>G. M. Schütz, "Exactly solvable models for many-body systems far from equilibrium," in *Phase Transitions and Critical Phenomena*, Vol. 19, edited by C. Domb and J. Lebowitz (Academic Press, London, 2001) pp. 1–251.
- <sup>31</sup>T. Chou, K. Mallick, and R. K. P. Zia, "Non-equilibrium statistical mechanics: from a paradigmatic model to biological transport," *Rep. Prog. Phys.* **74**, 116601 (2011).
- <sup>32</sup>A. Schadschneider, D. Chowdhury, and K. Nishinari, *Stochastic Transport in Complex Systems: From Molecules to Vehicles*, 3rd ed. (Elsevier Science, Amsterdam, 2010).
- <sup>33</sup>A. Scala, "Event-driven Langevin simulations of hard spheres," *Phys. Rev. E* **86**, 026709 (2012).
- <sup>34</sup>V. Ambegaokar and B. I. Halperin, "Voltage due to thermal noise in the dc Josephson effect," *Phys. Rev. Lett.* **22**, 1364–1366 (1969).
- <sup>35</sup>J.-P. Hansen and I. McDonald, *Theory of Simple Liquids* (Elsevier Science Publishers B.V., 1991).
- <sup>36</sup>J. K. Percus, "Equilibrium state of a classical fluid of hard rods in an external field," *J. Stat. Phys.* **15**, 505–511 (1976).
- <sup>37</sup>C. N. Likos, "Effective interactions in soft condensed matter physics," *Phys. Rep.* **348**, 267–439 (2001).
- <sup>38</sup>J. F. Lutsko, "Recent developments in classical density functional theory," in *Advances in Chemical Physics* (John Wiley & Sons, Ltd, 2010) Chap. 1, pp. 1–92.
- <sup>39</sup>R. Wittmann, M. Marechal, and K. Mecke, "Fundamental measure theory for non-spherical hard particles: predicting liquid crystal properties from the particle shape," *J. Phys.: Condens. Matter* **28**, 244003 (2016).
- <sup>40</sup>T. K. Vanderlick, H. T. Davis, and J. K. Percus, "The statistical mechanics of inhomogeneous hard rod mixtures," *J. Chem. Phys.* **91**, 7136–7145 (1989).
- <sup>41</sup>B. Bakhti, S. Schott, and P. Maass, "Exact density functional for hard-rod mixtures derived from Markov chain approach," *Phys. Rev. E* **85**, 042107 (2012).
- <sup>42</sup>A. Ryabov, D. Lips, and P. Maass, "Counterintuitive short uphill transitions in single-file diffusion," *J. Phys. Chem. C* **123**, 5714–5720 (2019).
- <sup>43</sup>D. Voráč, P. Maass, and A. Ryabov, "Cycle completion times probe interactions with environment," *J. Phys. Chem. Lett.* **11**, 6887–6891 (2020).